Computational Study of Enthalpy Probe Measurements in High-Speed Plasma Flow*

C. H. Chang and J. D. Ramshaw

Idaho National Engineering Laboratory
Idaho Falls, Idaho 83415
U. S. A.

The relative importance of various sources of error in enthalpy probe measurements in supersonic plasma flows have been assessed by means of detailed two-dimensional numerical simulations. The simulations show that moderate uncertainties in upstream pressure and composition can lead to significant errors in the velocity and temperature inferred from the measurements. Errors due to finite-rate ionization, internal electronic excitation, thermal radiation, probe cooling, and probe sampling were also investigated, and were not found to be significant under the conditions examined.

OVERVIEW

Despite their intrusive nature, enthalpy probes have been widely used for thermal plasma diagnostics due to their economy and ease of use [1–3]. Enthalpy probes can measure velocity by serving as a water-cooled Pitot tube, temperature or enthalpy by sampling, and gas composition by attachment to a mass spectrometer [1–3]. To date, most applications of this technique have been limited to flows at low Mach number. Recently, however, enthalpy probe measurements have been performed in high-speed (sonic and supersonic) plasma flows, and the results have generally shown good agreement with laser scattering techniques in the situations investigated [4]. However, the use of enthalpy probes under such conditions is subject to several possible sources of error which are insignificant or absent in low-speed flows and which are difficult to quantify experimentally. Our purpose here is to examine these errors by means of detailed two-dimensional simulations of high-speed plasma flows impinging on an enthalpy probe tip.

The enthalpy probe is only capable of measuring the total enthalpy h_t and the stagnation or total pressure p_t of the plasma. Assumptions are required to convert these quantities into the plasma velocity and temperature. Specifically, the unperturbed plasma is usually assumed to be in a state of local thermodynamic equilibrium (LTE) (which implies both thermal and chemical equilibrium) at the ambient pressure p_0, so

*Work performed under the auspices of the U. S. Department of Energy under DOE Field Office, Idaho, Contract DE-AC07-94ID13223, supported by the Office of Basic Energy Sciences, Division of Engineering and Geosciences, DOE-OER.

that the composition and degree of ionization are completely determined by the temperature [1–3]. The validity of this assumption is by no means obvious, as many of the important chemical reactions in plasmas are relatively slow three-body reactions with relatively long relaxation times. It is further assumed that h_t and p_t are related to the state of the unperturbed plasma by the simple analytic relations for isentropic frozen flow with constant specific heat ratio γ, combined in supersonic cases with shock jump conditions [4]. For subsonic cases one obtains [4,5]

$$\frac{p_1}{p_t} = \left(1 + \frac{\gamma - 1}{2} M_1^2\right)^{\gamma/(1-\gamma)} \tag{1}$$

while for supersonic cases [4,5]

$$\frac{p_1}{p_t} = \frac{[2\gamma M_1^2/(\gamma+1) - (\gamma-1)/(\gamma+1)]^{1/(\gamma-1)}}{[(\gamma+1)M_1^2/2]^{\gamma/(\gamma-1)}} \tag{2}$$

where p_1 and M_1 are respectively the static pressure and Mach number of the unperturbed (upstream) plasma. Since p_1 is not directly measured, it is generally assumed equal to p_0. The above equations determine M_1 in terms of p_t, and the "measured" velocity v_1 and temperature T_1 of the unperturbed plasma are then obtained from the relations $v_1 = M_1(\gamma R_g T_1)^{1/2}$ and $h_t = h_1 + v_1^2/2$, where R_g is the mixture gas constant and h_1 is the enthalpy of the unperturbed plasma, which is determined from T_1 by assuming equilibrium composition at T_1 and p_1.

This procedure embodies a number of assumptions, the validity of which is difficult to assess experimentally and which therefore represent potential sources of error. These potential errors include (1) deviations of p_1 from p_0, which are much more likely at the higher Mach numbers of present interest; (2) any deviations from equilibrium that may be present in the unperturbed plasma; (3) deviations from isentropic frozen flow due to finite-rate kinetics and associated departures from thermal equilibrium [6]; (4) deviations from adiabatic and stagnation conditions due to probe cooling and sampling; and (5) deviations from adiabatic flow at constant γ due to radiative energy loss and internal excitation.

This paper presents detailed numerical simulations of plasma flows impinging on an enthalpy probe tip in order to study the relative importance of the various sources of error discussed above. The present study is restricted to a laminar argon plasma flow for simplicity. Electrons, ions, and neutral atoms are represented as separate chemical species in the plasma mixture, and argon ionization/recombination by electron impact is represented by the kinetic chemical reaction $Ar + e^- \rightleftharpoons Ar^+ + e^- + e^-$, the rate for which is obtained from the two step model described by Hoffert and Lien [6]. All other reactions are neglected, since the third-body efficiency of electrons is much larger than that of heavy particles. Thermal nonequilibrium is represented by a conventional two-temperature model [7,8]. The simulations were performed using the LAVA computer code [7,9], which includes thermal nonequilibrium and ambipolar diffusion for multicomponent two-temperature plasmas [10]. The curved geometry of the enthalpy probe tip is modeled by the use of an excluded volume or porosity function to represent the fraction of each cell volume and cell face area which is available to the flow [8]. A detailed discussion of the fluid dynamical aspects of the model is given elsewhere [7–9].

RESULTS AND DISCUSSION

The calculational region is 3 cm radially by 4 cm axially, and is subdivided by a nonuniform 80×79 computational mesh. The geometry is axisymmetric, so the simulations were performed in two-dimensional cylindrical coordinates. The left boundary is the symmetry axis, and the flow is upward. The bottom boundary is the inflow boundary, at which the velocity, temperature, and pressure are uniform. The top and right boundaries are open boundaries.

The enthalpy probe is modeled as a circular cylinder with hemispherical cap as shown in Fig. 1. The enthalpy probe hole has a radius of $R_0 = 0.5$ mm, and is comprised of the leftmost five computational cells at the probe tip. The total pressure p_t is obtained from the pressure at the stagnation point. The total enthalpy h_t is obtained as the mass-weighted average of the total enthalpy in the five cells at the probe tip. We performed a set of supersonic flow simulations under various different conditions as described below. In all cases, local thermal equilibrium (*i.e.*, $T = T_e$) is assumed at the inflow.

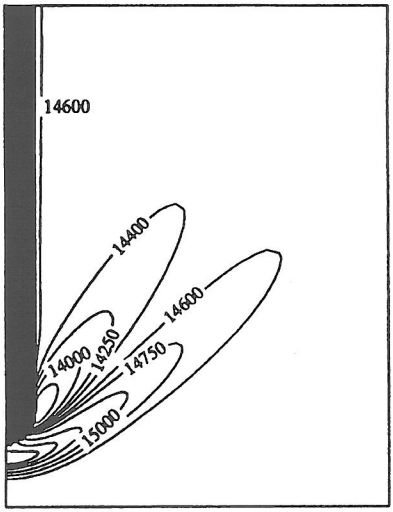

Fig. 1. Heavy particle temperature field in the base case. The high contour value is 16,500 K, the low value is 13,500K, and the interval between unlabeled contours is 500K.

The base supersonic case is one in which there are no uncertainties in upstream pressure or composition. The specified inflow conditions are $v_1 = 3600$ m/s, $T_1 = 14500$ K, $p_1 = 85.2$ kPa, $M_1 = 1.31$, and complete LTE. (All Mach numbers used in this paper are based on the frozen speed of sound.) Finite-rate ionization kinetics is included.

The resulting computed heavy particle temperature field in steady state is shown in Fig. 1. The electron temperature field is visually almost indistinguishable from Fig. 1 except near the probe tip. The corresponding pressure field is shown in Fig. 2, which shows the shock wave in front of the probe and the expansion wave near the beginning of the straight section of the probe.

Heavy particle and electron temperatures and pressure along the axis are shown in Fig. 3. Due to the ionization behind the shock wave, which absorbs electron energy, the electron temperature drops slightly below the heavy particle temperature, as previously observed [6]. The temperatures in the region near the stagnation point then further decrease as ionization continues to proceed, while the pressure monotonically increases as the stagnation point is approached.

Figure 4 shows the electron density and degree of nonequilibrium along the axis. The degree of nonequilibrium is defined as $\zeta = K_{eq}^{-1}[\mathrm{Ar}^+][e^-]/[\mathrm{Ar}]$, where [X] is the molar concentration of species X in the plasma, and K_{eq} is the equilibrium constant for

ionization, evaluated at the electron temperature. As the temperature increases, the plasma becomes under-ionized in a manner consistent with the finite-rate chemistry. As the plasma approaches the stagnation point, however, the fluid dynamical time scales become longer due to the reduced flow speed, while the chemical (ionization) time scale becomes shorter due to the higher temperature and electron density. The ionization consequently catches up with the temperature change and the plasma returns closer to equilibrium. This additional ionization takes up some thermal energy, thereby resulting in the temperature reductions observed in Fig. 3.

In this calculation, the computed values of h_t and p_t yield "measured" values of $T_1 = 14454$ K and $v_1 = 3623$ m/s, which are in very good agreement with the specified inflow values, in spite of the use of frozen relations in a flow with finite-rate chemistry. Further investigation [8] indicates that this agreement results from a rather counterintuitive insensitivity to the effects of finite-rate chemistry.

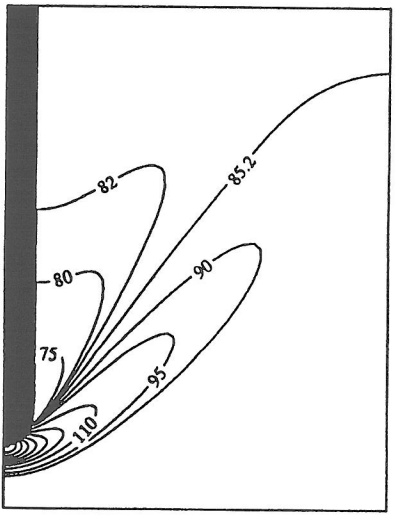

Fig. 2. Pressure field in the base case. The high contour value is 230 kPa, and the interval between unlabeled contours is 20 kPa.

The effect of upstream pressure uncertainty was examined by simulating cases identical to the base case except for the upstream pressure, which was set to values of $p_1 = 1.2\ p_{amb}$ and $p_1 = 0.9\ p_{amb}$. The "measured" upstream temperatures and velocities obtained from the computed h_t and p_t were $T_1 = 14158$ K, $v_1 = 3972$ m/s in the former case, and $T_1 = 14622$ K, $v_1 = 3421$ m/s in the latter. Note that the upstream pressure errors lead to larger errors in velocity than temperature.

The effect of chemical nonequilibrium in the upstream plasma was examined by simulations identical to the base case except for upstream composition. The equilibrium mole fractions of argon plasma at 14500 K and 85.2 kPa are $[Ar]:[Ar^+]:[e^-] = 0.308:0.346:0.346$, resulting in an equilibrium molar concentration ratio $\xi_{eq} = [Ar^+]/[Ar] = 1.123$. In the under-ionized case, we set $\xi = 0.2\xi_{eq}$, resulting in mole fractions of $[Ar]:[Ar^+]:[e^-] = 0.690:0.155:0.155$, while in the over-ionized case we set $\xi = 5\xi_{eq}$, resulting in mole fractions of $[Ar]:[Ar^+]:[e^-] = 0.082:0.459:0.459$. In these cases, the temperature and velocity of the unperturbed plasma vary with axial distance, since the ionization reaction progresses as the plasma flows downstream. Values of v_1 and T_1 obtained by the enthalpy probe relations must therefore be compared to the temperature and velocity at the position of the enthalpy probe hole in the absence of the probe. In order to minimize the relaxation back to ionization equilibrium, the inflow boundary was moved closer to the probe (0.2 cm) in these simulations.

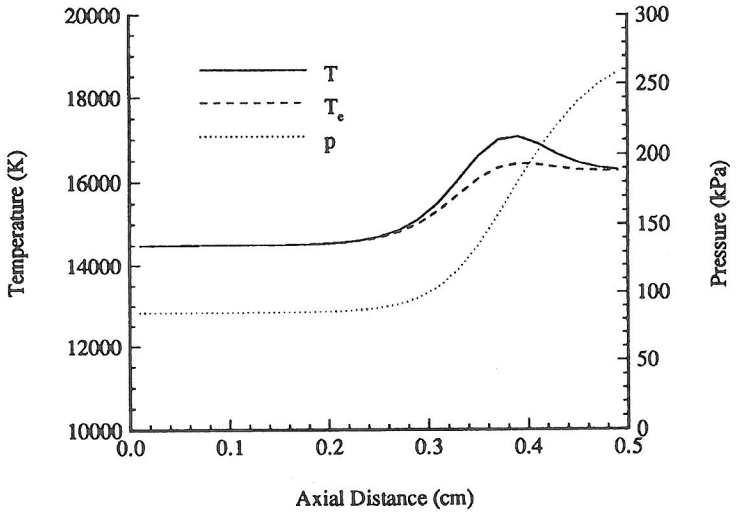

Fig. 3. Heavy particle temperature, electron temperature, and pressure along the centerline in the base case.

In the under-ionized case, the true heavy particle temperature, electron temperature, and velocity at the probe location with the probe absent are $T = 13335$ K, $T_e = 13052$ K, and $v = 3691$ m/s, while the "measured" values are $T_1 = 12705$ K and $v_1 = 3407$ m/s. In the over-ionized case, the true heavy particle temperature, electron temperature, and velocity are $T = 16438$ K, $T_e = 16435$ K, and $v = 3406$ m/s, while the "measured" values are $T_1 = 16074$ K and $v_1 = 3922$ m/s. We again observe that the temperature errors are smaller than the velocity errors.

The effects of radiation heat loss, internal excitation, probe cooling, and probe sampling were also assessed by calculations similar to those described above. These effects were not found to be significant under the conditions examined [8].

CONCLUDING REMARKS

Even though these calculations are limited to argon plasmas, we would expect plasmas of other monatomic gases and gas mixtures to behave similarly. However, in diatomic gases, large changes in γ occur due to vibrational excitation and dissociation. This may lead to larger probe measurement errors than in monatomic gases.

The present study was restricted to uniform free stream conditions for simplicity. In contrast, supersonic plasma jets used in processing have steep radial gradients and can possess complex flow structures such as oblique shocks and expansion waves. Enthalpy probe measurements in these situations are potentially subject to additional sources of error not investigated in this paper. We hope to investigate these effects in a future study.

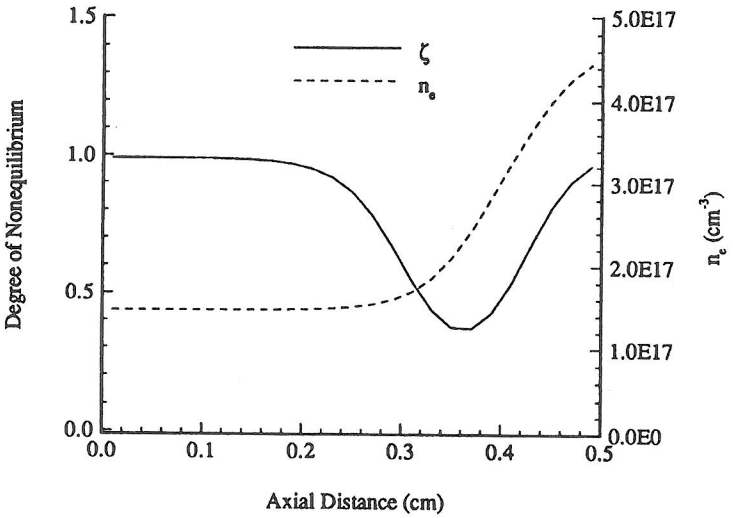

Fig. 4. Electron density and degree of nonequilibrium along the centerline in the base case.

Our simulations indicate that enthalpy probes should generally produce good results even in supersonic flows with chemical reactions, provided that reasonable estimates of the upstream pressure and degree of ionization are available. In the cases examined by Fincke *et al.* [4], the upstream pressure and degree of ionization were evidently close to the assumed values. When they are not, however, the potential for significant error exists, and enthalpy probe users should be aware of this.

REFERENCES

1. M. Brossa and E. Pfender, *Plasma Chem. Plasma Process.* **8**, 75 (1988).
2. A. Capetti and E. Pfender, *Plasma Chem. Plasma Process.* **9**, 329 (1989).
3. J. R. Fincke, C. H. Chang, W. D. Swank, and D. C. Haggard, *Int. J. Heat Mass Transfer* **37**, 1673 (1994).
4. J. R. Fincke, W. D. Swank, S. C. Snyder, and D. C. Haggard, *Rev. Sci. Instrum.* **64**, 3585 (1993).
5. S. Schreier, *Compressible Flow*, Wiley, New York (1982).
6. M. I. Hoffert and H. Lien, *Phys. Fluids* **10**, 1769 (1970).
7. C. H. Chang and J. D. Ramshaw, *Phys. Plasmas* **1**, 3698 (1994).
8. C. H. Chang and J. D. Ramshaw, "Computational Study of High-Speed Plasma Flow Impinging on an Enthalpy Probe," *Plasma Chem. Plasma Process.* (accepted).
9. J. D. Ramshaw and C. H. Chang, *Plasma Chem. Plasma Process.* **12**, 299 (1992).
10. J. D. Ramshaw and C. H. Chang, *Plasma Chem. Plasma Process.* **13**, 489 (1993).